Imperial College London

CO$_2$ Reduction in Micro-tubular Solid Oxide Electrolysers

Lisa Kleiminger, Tao Li, Kang Li and Geoff H. Kelsall.

Department of Chemical Engineering, Imperial College London, London SW7 2AZ, UK.

INTRODUCTION

Electrochemical reduction of CO_2 and/or H_2O to produce CO and/or H_2 could provide the basis of large-scale energy storage to smooth the dynamics of renewable power sources and electrical power demands (Figure 1), and if operated with renewable power sources, could mitigate CO_2 emissions from e.g. steel and cement production.

Micro-tubular solid oxide electrolysers and fuel cells are robust to thermal cycling, have fast start-up, facile to seal [3,4], and their volumetric power densities ($\propto \pi/d$) increase with decreasing tube diameter (d), so exceeding the values for planar structures.
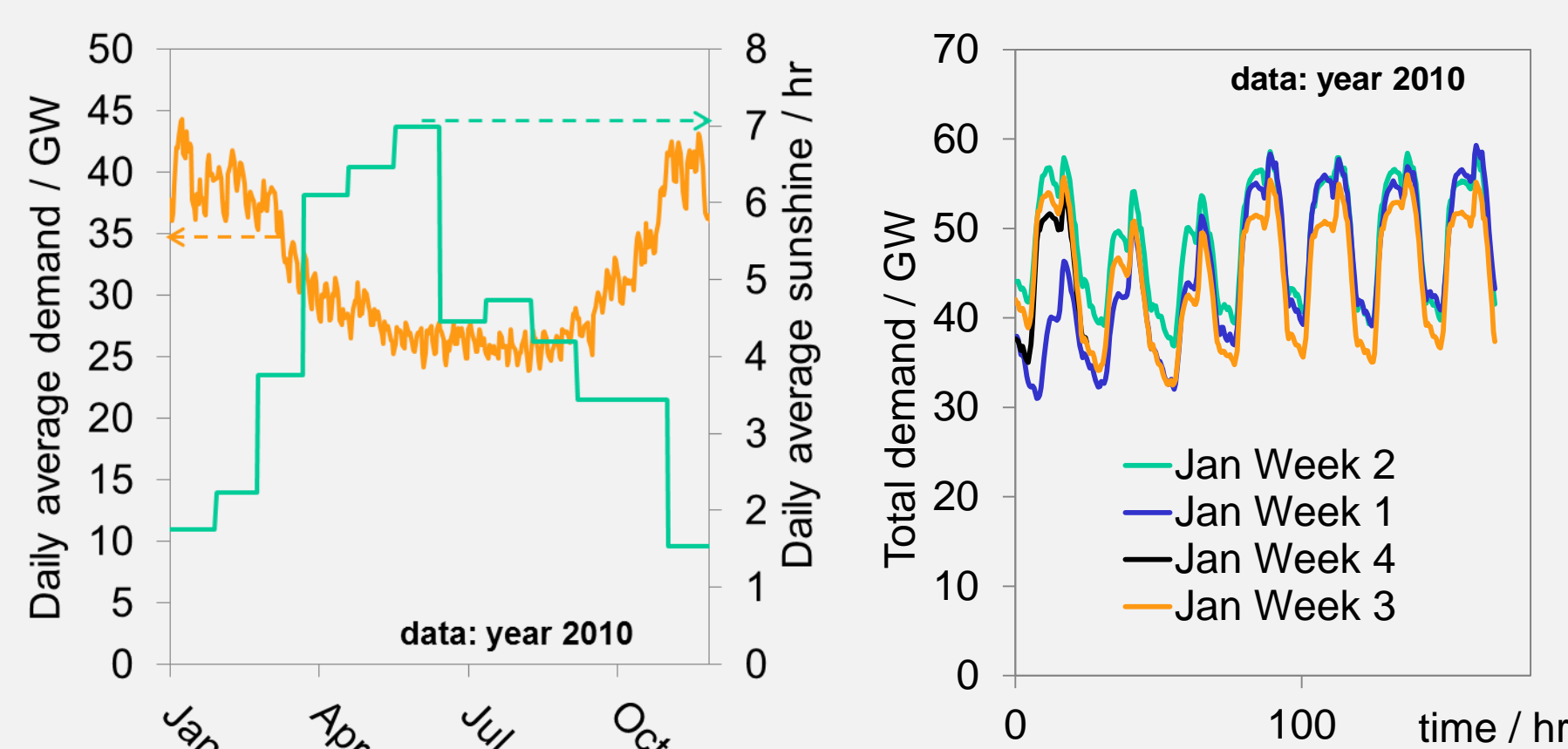

Figure 1: Seasonal (daily average) and weekly (daily variation) UK power demand [1, 2].

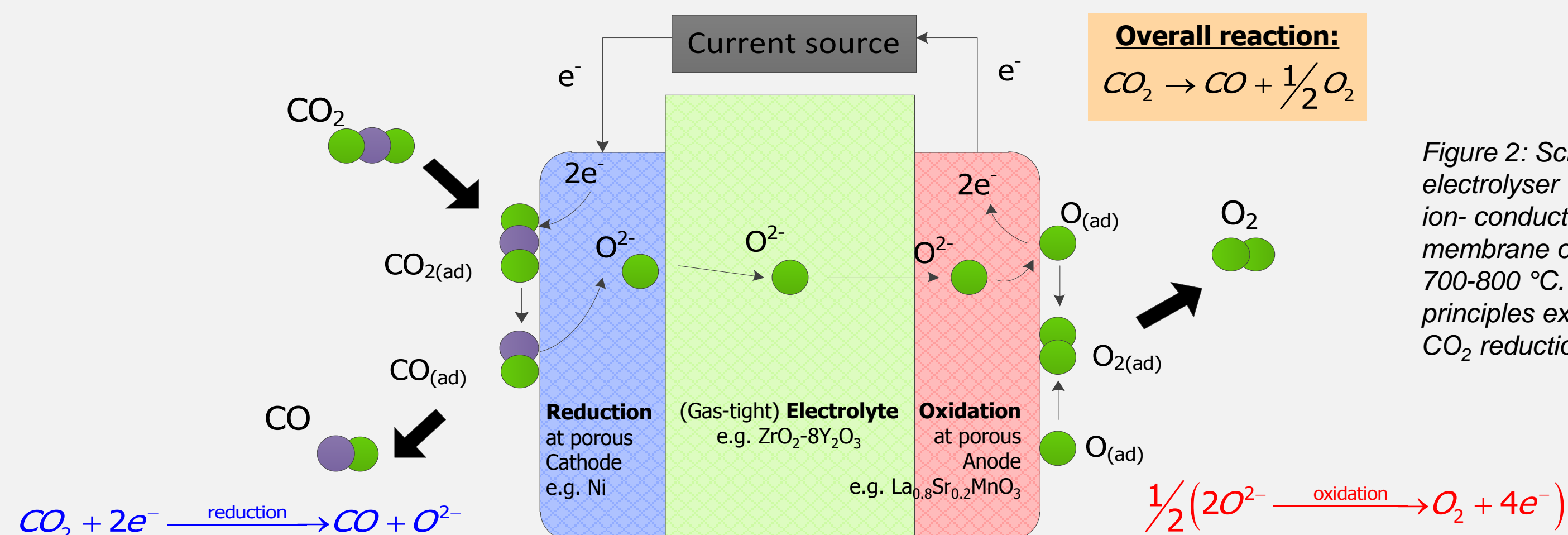## SOLID OXIDE ELECTROLYSER REACTIONS

Overall reaction:
$$CO_2 \rightarrow CO + \tfrac{1}{2}O_2$$

Figure 2: Schematic of electrolyser with oxide ion- conducting membrane operating at 700-800 °C. Working principles explained for CO_2 reduction.

Reduction at porous Cathode e.g. Ni

(Gas-tight) Electrolyte e.g. ZrO_2-$8Y_2O_3$

Oxidation at porous Anode e.g. $La_{0.8}Sr_{0.2}MnO_3$

$$CO_2 + 2e^- \xrightarrow{reduction} CO + O^{2-}$$

$$\tfrac{1}{2}\left(2O^{2-} \xrightarrow{oxidation} O_2 + 4e^-\right)$$

REACTOR FABRICATION

Electrolysers of the form Ni-YSZ|YSZ|YSZ-LSM|LSM (Figure 3) were prepared in two-steps (with YSZ = 8 Y_2O_3-ZrO_2 and LSM = $La_{0.8}Sr_{0.2}MnO_3$):

- Dual-layer co-extrusion phase inversion to produce Ni-YSZ|YSZ hollow fibre precursors (co-sintered at 1500 °C – 10 hours)
- Brush-coating of LSM-YSZ|YSZ layers followed (sintered at 1100 °C – 3 hours).

Figure 4: Phase inversion system to fabricate dual-layer hollow fibre precursors.
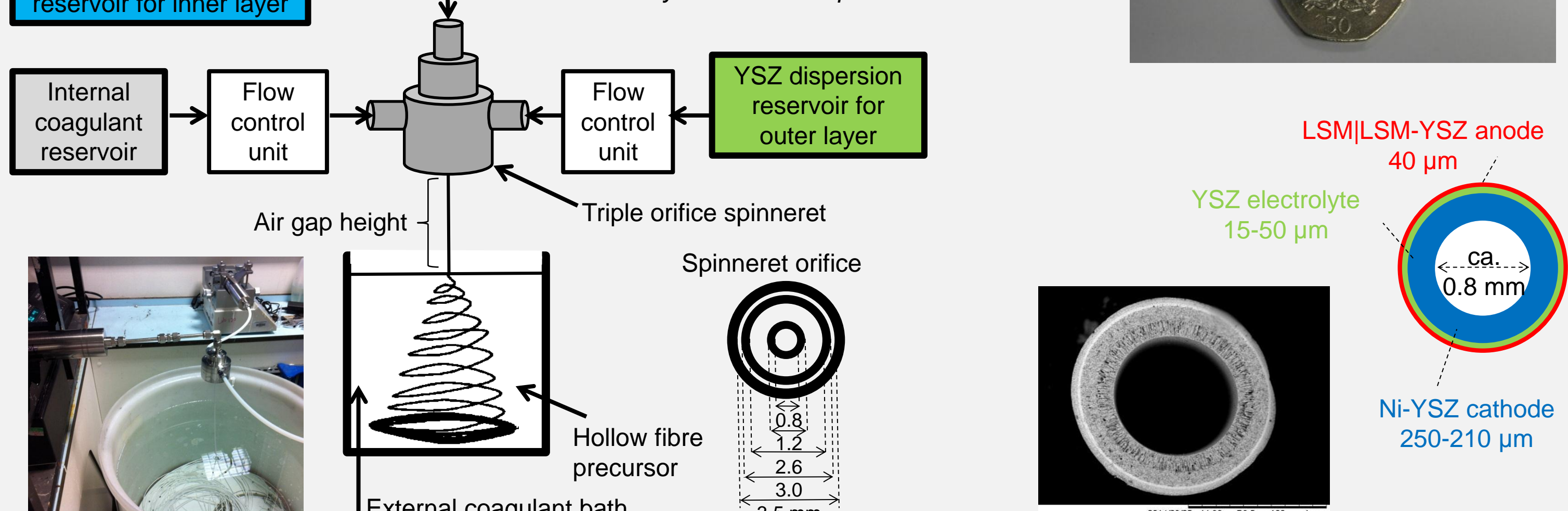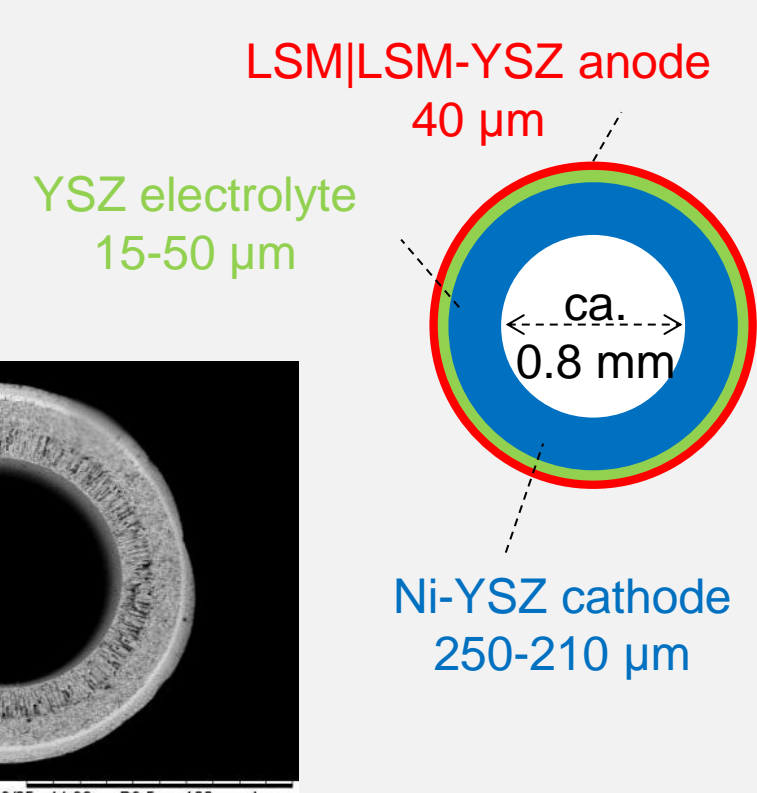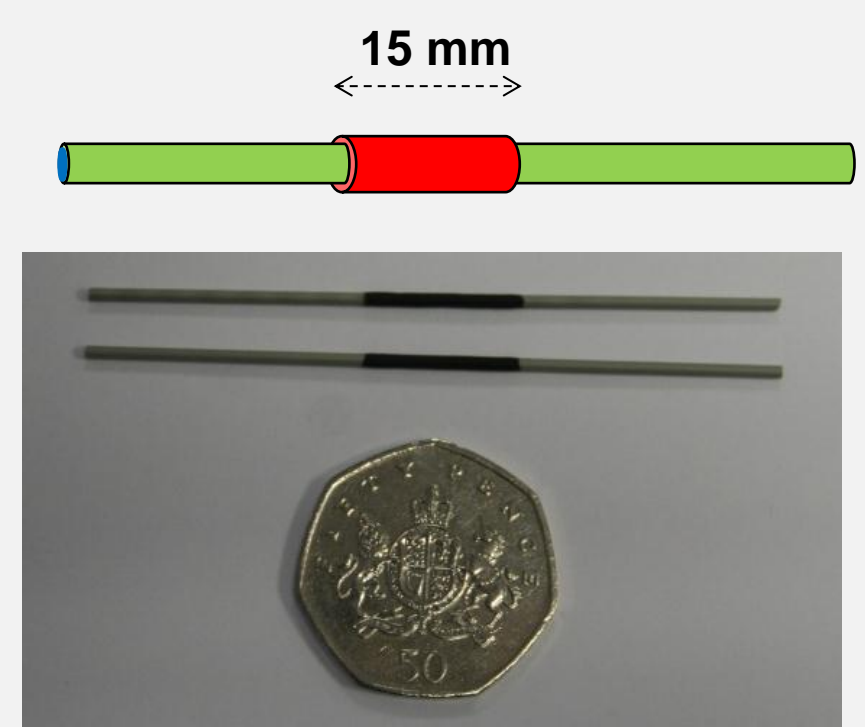

Figure 3: Reactor geometry — 15 mm

LSM|LSM-YSZ anode 40 μm
YSZ electrolyte 15-50 μm
ca. 0.8 mm
Ni-YSZ cathode 250-210 μm

Figure 5: Scanning electron micrographs of (reduced) cross-sectioned fibres (post-operation) with varying electrolyte thickness.

49μm   26 μm   19 μm

LSM   LSM-YSZ   YSZ   Ni-YSZ

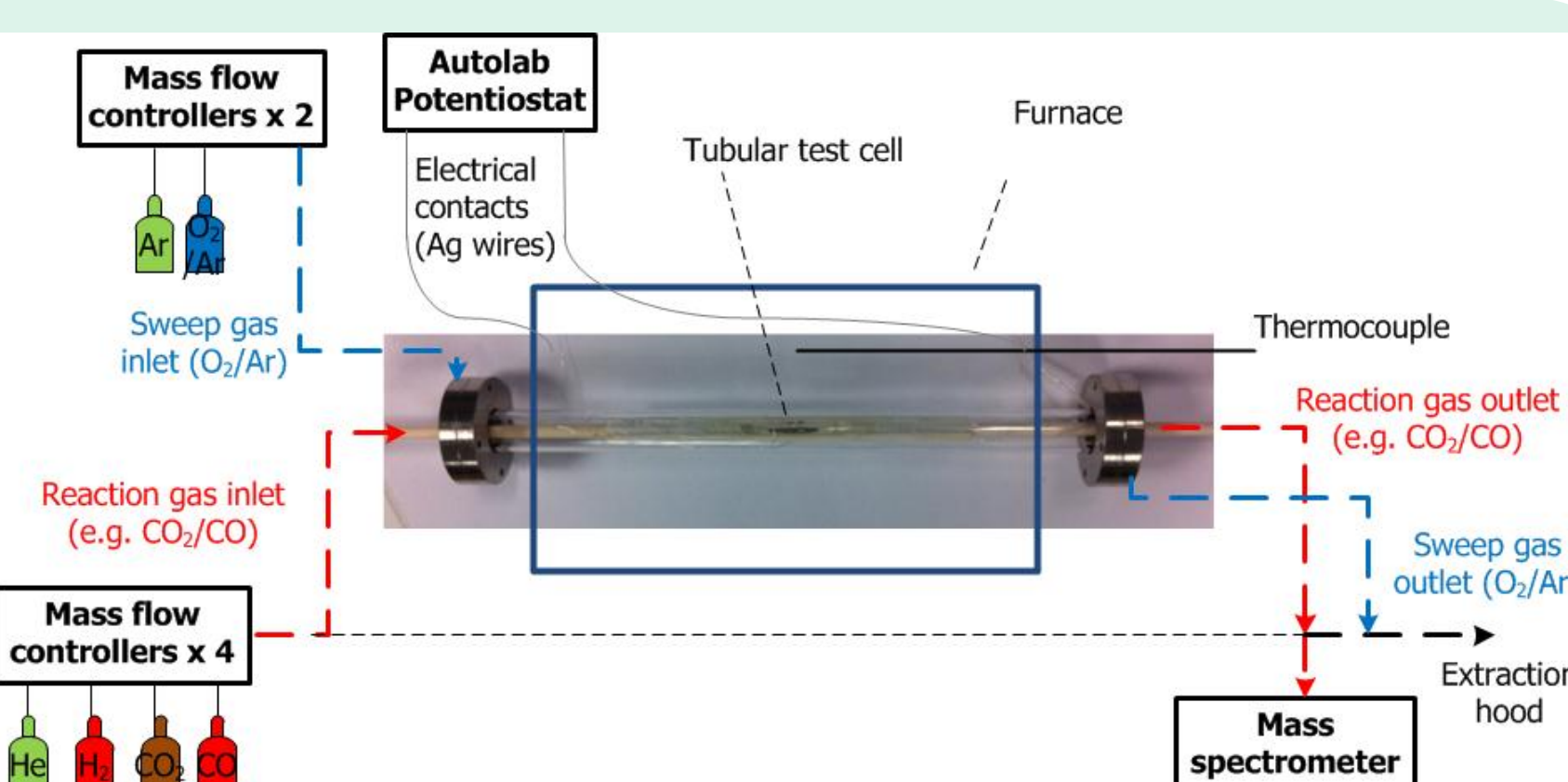## ELECTROLYSIS PERFORMANCE: CO$_2$ REDUCTION

Figure 6: Schematic of experimental equipment.
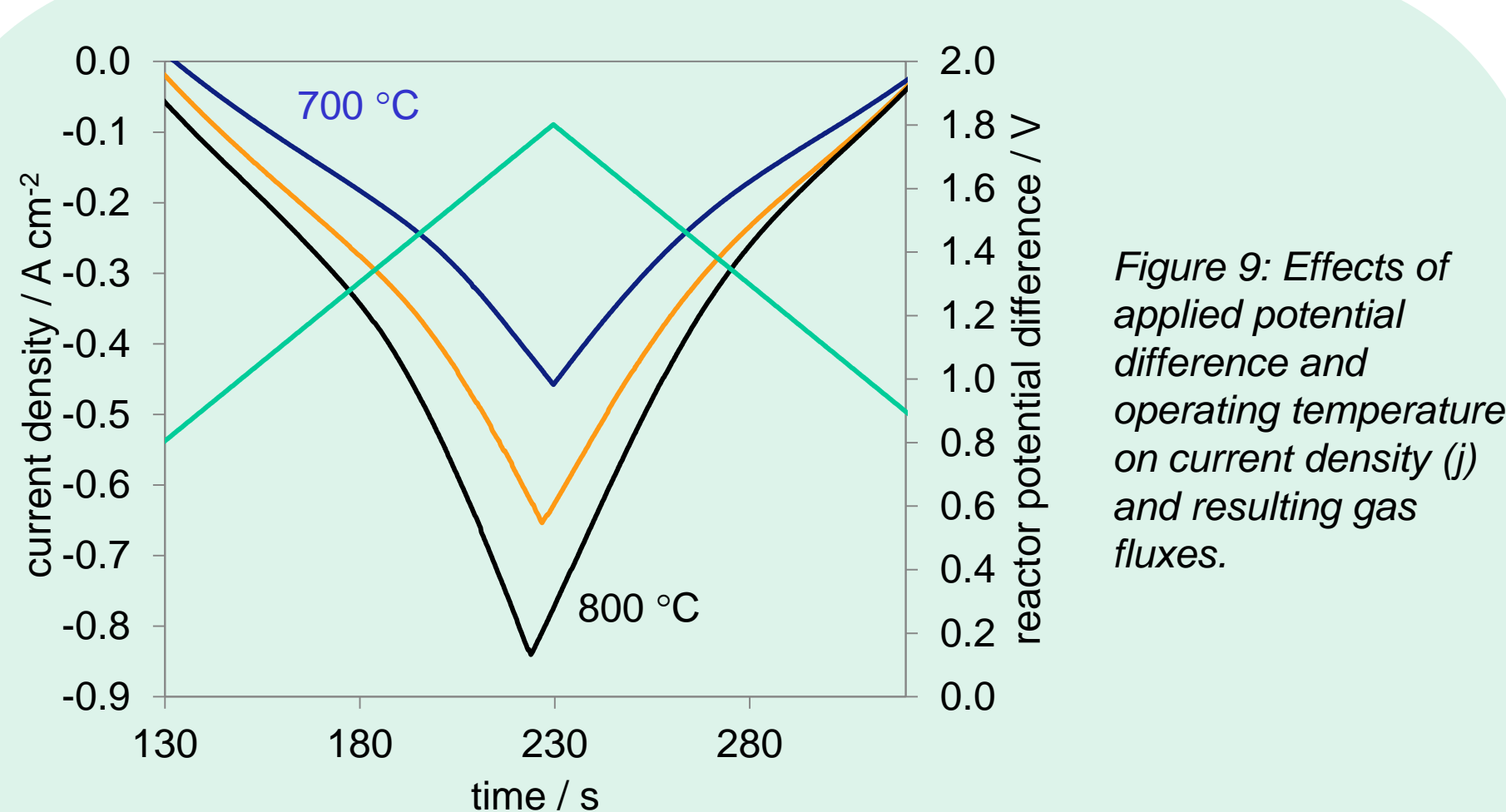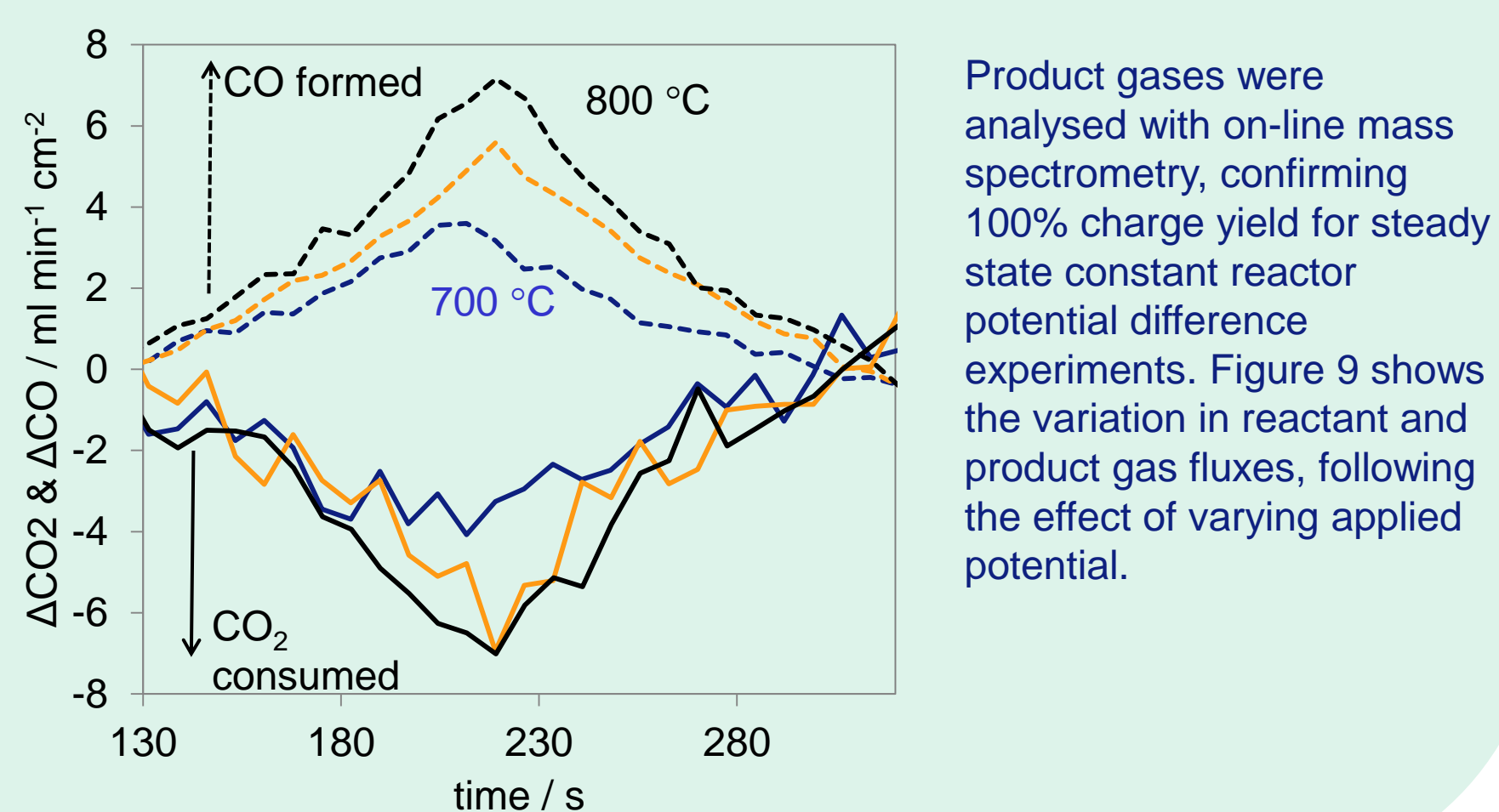
Figure 9: Effects of applied potential difference and operating temperature on current density (j) and resulting gas fluxes.

Product gases were analysed with on-line mass spectrometry, confirming 100% charge yield for steady state constant reactor potential difference experiments. Figure 9 shows the variation in reactant and product gas fluxes, following the effect of varying applied potential.

Increasing operating temperature and decreasing electrolyte thickness enhanced electrolyser performance. (Figure 7). Temperature both increases electrolyte conductivities (1.9 to 4.3 S m-1 for 700-800 °C, respectively [5]) and enhances electrode kinetics.

Specific electrical energy consumption
$$w^e_{CO_2}/kW\,h\,(t\,CO_2)^{-1} = \frac{2F}{\Phi^e_{CO_2}} \cdot \frac{U}{3.6 M_{CO_2}}$$

Market price:	£ 700 per tonne CO
	£ 40 per tonne O_2
Energy cost:	£ 140-350 per tonne CO

Figure 7: Effects of applied current density (j) and operating temperature/ electrolyte thickness on cell potential difference (U) and specific electrical energy consumption (w_e) at 90/10 CO_2/CO gas feed composition.

Strong dependence of total area specific resistance (ASR) as a function of the current density/ cell potential difference derived from change in slopes of the j-U curves (Figure 7) has been observed. Change in ASR believed to be a result of endothermic nature of CO_2 reduction versus Joule heating resulting in a minimum temperature (peak ASR around 1.0-1.2 V) between the open circuit and thermo-neutral potential difference (ca. 1.46 V).

Figure 8: Effects cell potential difference and temperature on ASR for 50 μm thick electrolyte and 90/10 CO_2/CO gas feed.

Analysis of the ohmic resistance ($\Delta\phi^{IR}_{total} = \int^{r_e+t_e}_{r_e} \frac{j(r)}{\sigma_e}dr + \frac{I_{cell}l_{wire}}{A_{wire}\sigma_{wire}} + \Delta\phi^{IR}_{contact} + \int^{r_c}_{r_c+t_c} \frac{j(r)}{\sigma_{Ni\,electrode}}dr + \int^{r_a+t_a}_{r_a} \frac{j(r)}{\sigma_{LSM\,electrode}}dr$), based on impedance spectroscopy (Figure 10), revealed that electrolyte resistance contributed only 28-5% (50-15 μm / 700-800 °C) towards the total, the remaining losses being associated with the wires (⅓) and contact losses (⅔) – Figure 11.
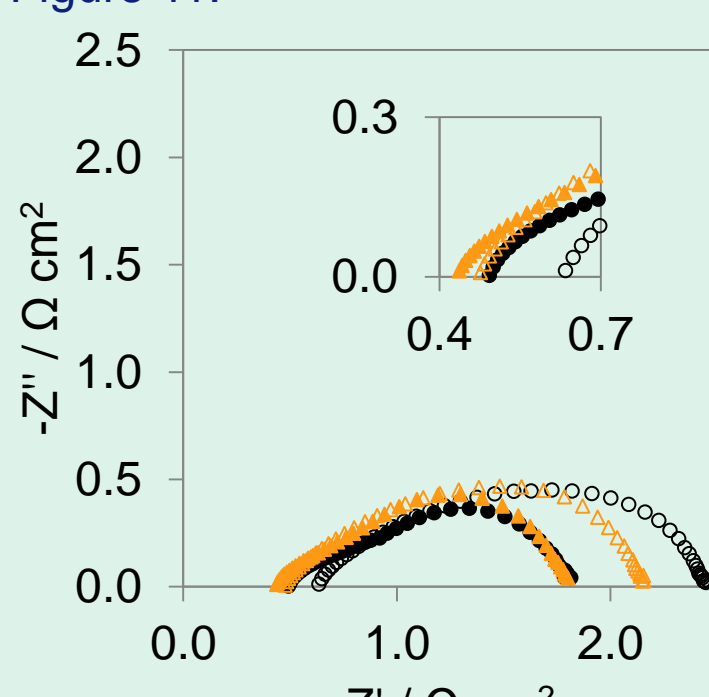
Figure 10: Electrical impedance spectra at 700 °C (unfilled) and 800 °C (filled) for electrolyte thickness extremes: 15 (▲) and 50 (●) μm measured at open circuit potential difference.
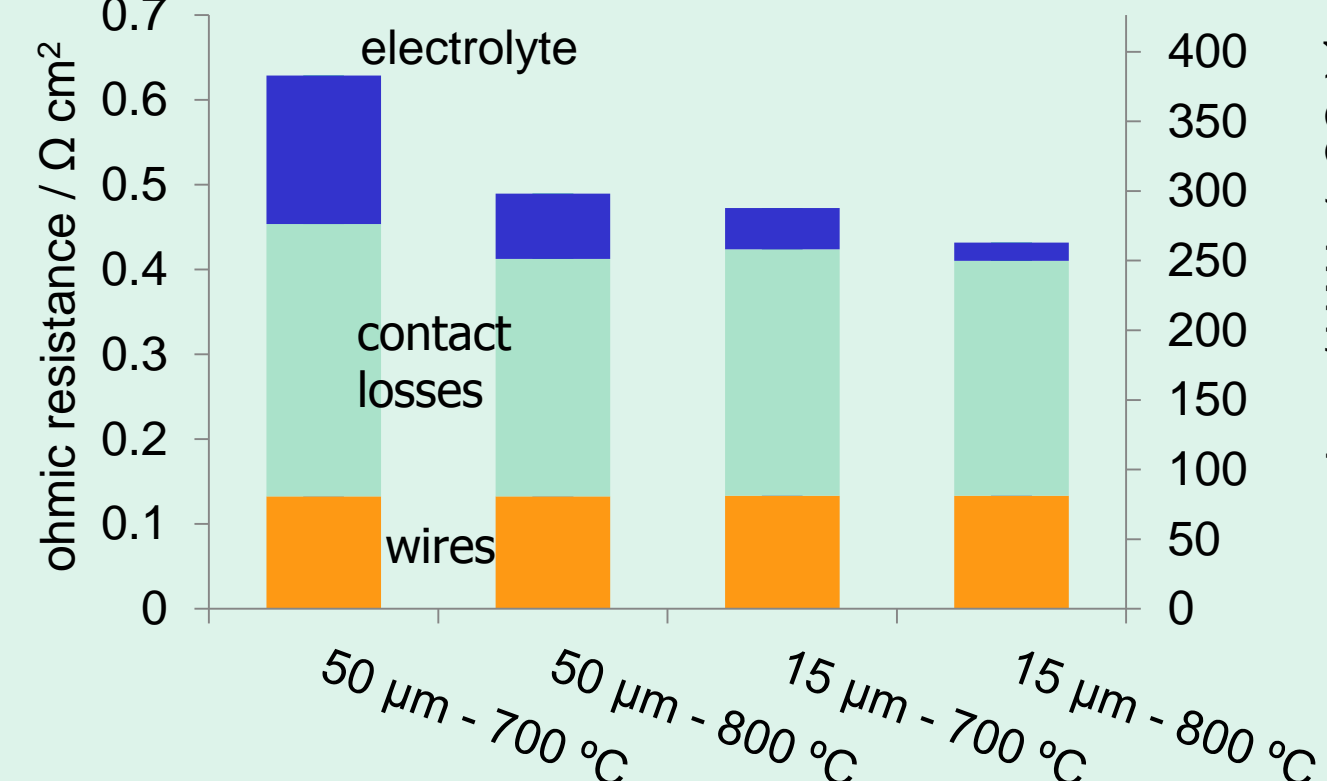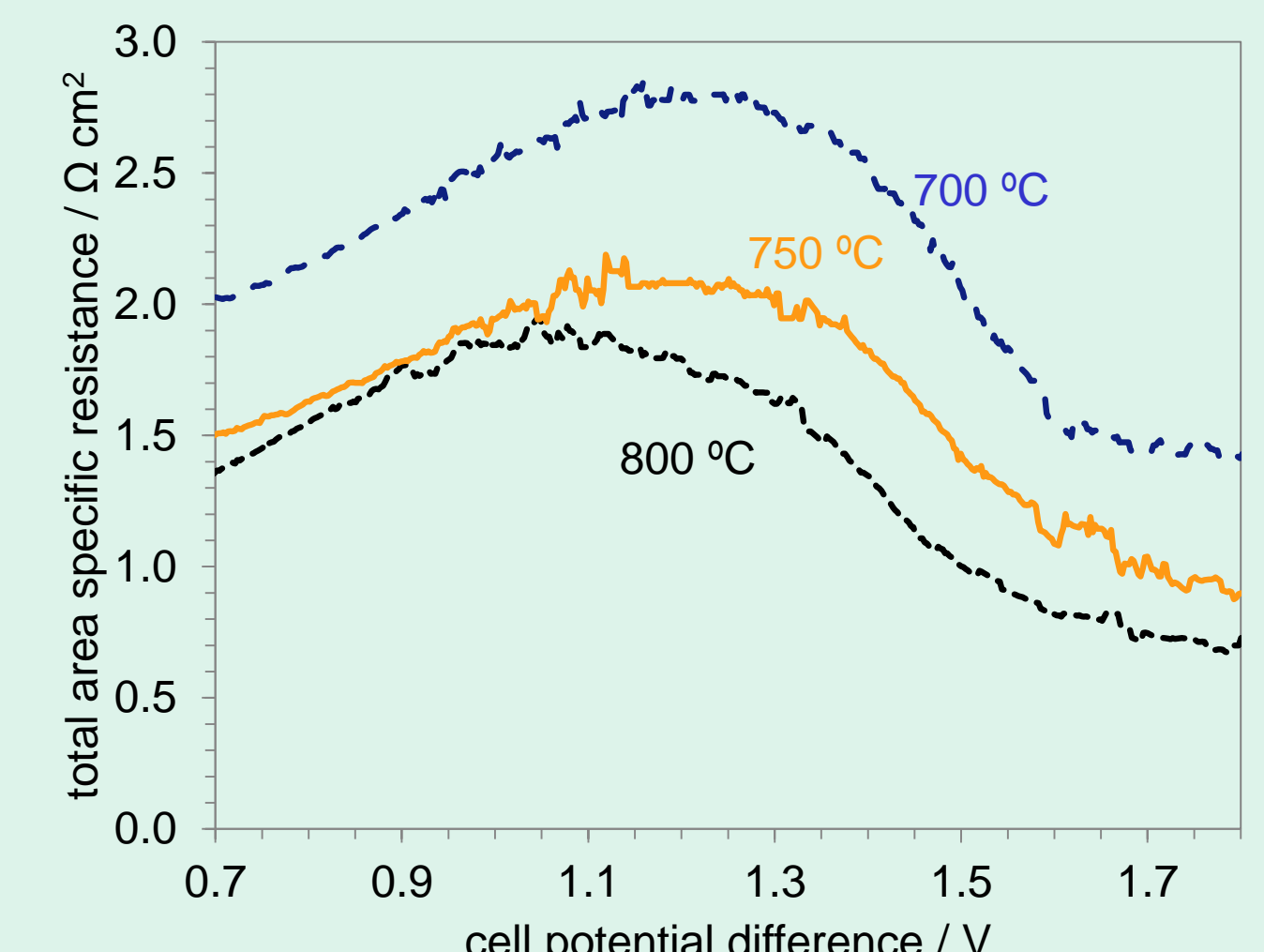
Figure 11: Individual contributions to ohmic resistance as a function of temperature and electrolyte thickness.

50 μm - 700 °C   50 μm - 800 °C   15 μm - 700 °C   15 μm - 800 °C

Reversibility of operating the solid oxide reactor in electrolyser (energy storage) and fuel cell (power re-generation) mode was demonstrated. Round-trip efficiencies of 72-32 % for 0.1-0.3 A cm⁻² at 800 °C were achieved.
However, different gas feed compositions for electrolysis and fuel cell mode would be required to optimize reactor performance.
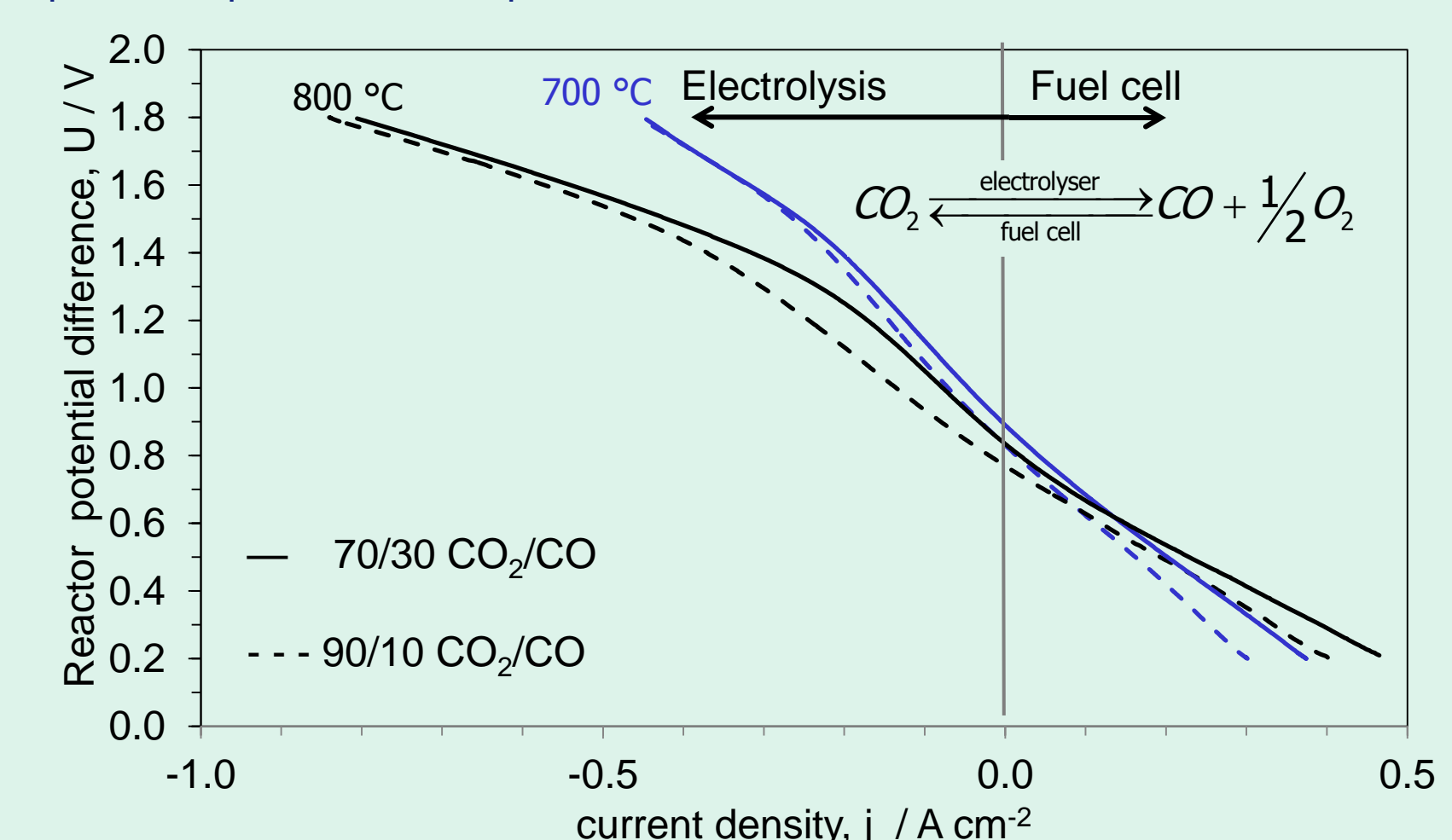
$$CO_2 \underset{fuel\,cell}{\overset{electrolyser}{\rightleftharpoons}} CO + \tfrac{1}{2}O_2$$

— 70/30 CO_2/CO
--- 90/10 CO_2/CO

Figure 12: Effects of applied current density (j) and operating temperature on cell potential difference (U) using a 50 μm thick electrolyte for different CO_2/CO gas feed compositions.

The oxide ion flow across the anode|electrolyte|cathode cross-section during electrolysis has been visualized using isotopic labelled $C^{18}O_2$ and Secondary Ionic Mass Spectrometry (SIMS).
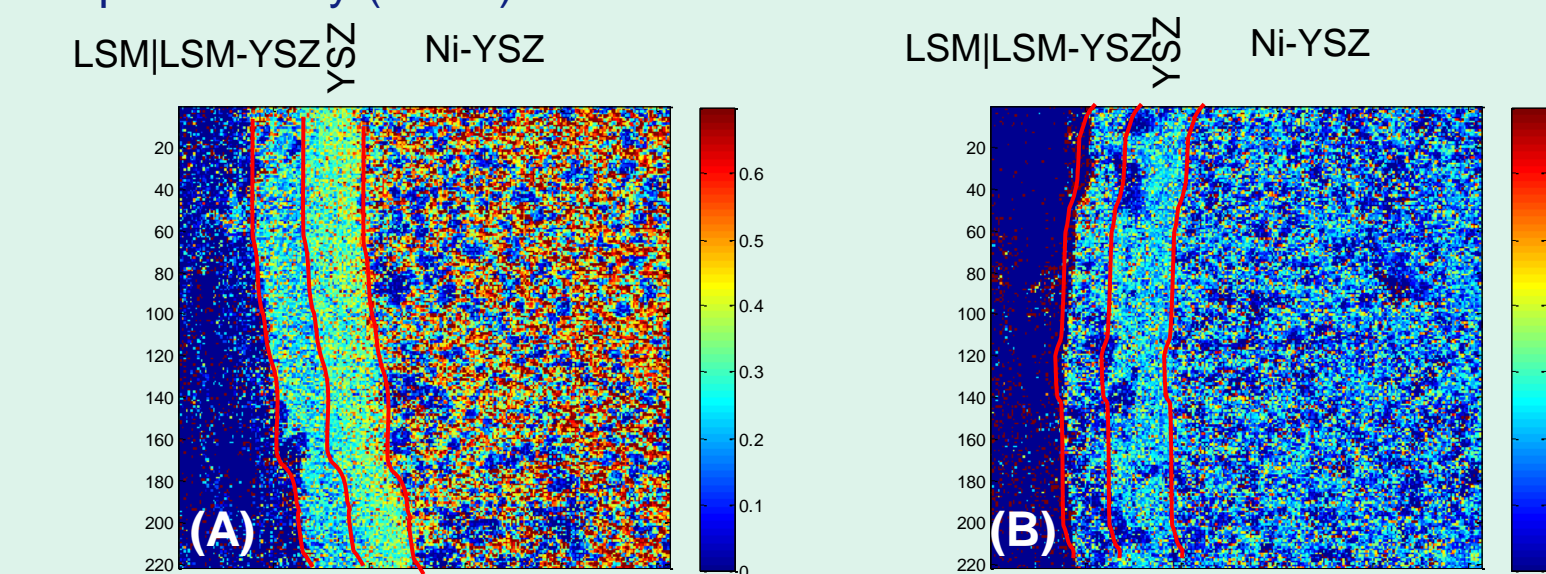
LSM|LSM-YSZ   Ni-YSZ

Figure 13: Oxygen-18 fraction map of anode|electrolyte|cathode cross-section at j=0.27 A cm⁻² for 30 seconds (A) and open circuit potential difference (B). Hollow fibre reactors operated simultaneously.

SUMMARY & FUTURE WORK

- Successful fabrication of Ni-YSZ|YSZ|LSM-YSZ|YSZ micro-tubular electrolysers using dual-layer phase inversion and sintering
- Maximum performance of 1.0 A cm⁻² at 1.8 V in CO_2 electrolysis mode for 15 μm thick electrolyte
- Wires (21-31 %) and contact losses (51-64 %), rather than the electrolyte itself (28-5%) were major contributors to ohmic losses
- Reactors can be operated reversibly (electrolyser and fuel cell mode)
- The oxide ion flow within the electrolyte could be visualized.
- Ways to minimize the contact losses and long-term degradation are currently being investigated.
- Comparison between H_2O and CO_2 electrolysis: up to 68 % (800 °C) performance enhancement for H_2O and co-electrolysis compared with reduction of CO_2 alone.

ACKNOWLEDGEMENTS & REFERENCES

[1] Met Office: http://www.metoffice.gov.uk/climate/uk/2010/ [accessed June 2014].
[2] National Grid: http://www2.nationalgrid.com/uk/industry-information/Electricity-transmission-operational-data/Data-Explorer/ [accessed June 2014].
[3] K. Kendall, Int. J. Appl. Ceram. Technol., 2010, 7, 1.
[4] Y. Du, N.M. Sammes, J. Power Sources, 2004, 136, 66.
[5] H. Zhu, R.J. Kee, J. Power Sources, 2003, 117, 61.